

Female House Mice Develop a Unique Ovarian Lesion in Colonies That Are at Maximum Population Density (44555)

JOHN C. CHAPMAN, JOHN J. CHRISTIAN,² MARY ANN PAWLIKOWSKI, NORIE YASUKAWA,² AND SANDRA D. MICHAEL¹

Department of Biological Sciences, Binghamton University, Binghamton, New York 13902-6000

Abstract. Colonies of house mice reach maximum population density in 120–180 days, irrespective of cage size and initial number of colonizing animals. Reproduction ceases because the females become aggressive and unreceptive to mating. The aggressive behavior is correlated with elevated levels of testosterone (T) and corticosterone (B) (Chapman *et al.*, *Phys Behav* 64:529–533, 1998). In two of seven strains of mice, females developed ovarian lesions. The occurrence of the lesion in one strain was correlated with the age of the animal and duration of the study. In the second strain, cage size was the determining factor. Lesioned ovaries weighed significantly more than nonlesioned ovaries. The lesion consisted of accumulations of luteal membrane and organelle fragments, and other cellular debris, suggestive of incomplete and prolonged luteolysis. Electron microscopic (EM) analyses revealed the presence of deposits of permanganate-resistant congophilic amyloid fibrils in the intima and smooth muscle cells of luteal thecal arteries.

Population females had thymus glands and uteri that weighed significantly less than the same organs from females housed in the breeding colony, whereas the adrenal glands from the population females weighed significantly more.

It is proposed that the female aggression is due to high levels of T. It is also proposed that the high levels of B suppress the immune cells involved in normal luteolysis and contribute to the incomplete and prolonged luteolysis.

[P.S.E.B.M. 2000, Vol 225:80–90]

Previous laboratory studies on the reproductive behavior of the house mouse (*Mus musculus*) have determined that population size is controlled by the female (1, 2). In a typical mouse population, the females mate during an early growth phase, become repeatedly pregnant, and subsequently bear and maintain their litters. As population density increases, the females undergo a change in reproductive behavior and begin to exhibit signs of male-like aggression. The change in behavior occurs as each population approaches its maximum size. Similar-sized mouse populations consisting of all females rarely exhibit this aggressive behavior. However, when a male is added to

the assemblage, and reproduction is involved, the aggressive nature of the females is displayed.

Females that reach high population density have levels of circulating testosterone (T) that are six- to seven-fold higher than the values found in female mice housed separately in a breeding colony (3). Moreover, the levels of corticosterone (B) in these animals approach those found in stressed mice (4). The highest levels of B, most notably, are in the youngest females of the population.

In addition to the aggressive behavior and their high levels of T and B, females in high-density populations also develop a unique ovarian lesion. The lesion originates in corpora lutea and appears as an amorphous white mass consisting of accumulations of membrane fragments and other cellular debris, suggestive of incomplete and prolonged luteolysis. Electron microscopic (EM) analyses indicates that the lesions contain deposits of amyloid fibers that are localized in the cells of the hilar/thecal arteries and in adjacent luteal cells. The amyloid fibers are characterized as a primary, permanganate-resistant entity, and are unrelated to secondary amyloidosis (amyloid protein A amyloidosis). Previous descriptions of ovarian amyloidosis in house mice have been restricted to reports of the amyloid found in old

This work was supported by NIH grant HD2336203.

¹ To whom requests for reprints should be addressed at the Department of Biological Sciences, Binghamton University, Binghamton, NY 13902-6000. E-mail: smichael@binghamton.edu

² Deceased.

Received November 3, 1999. [P.S.E.B.M. 2000, Vol 225]

Accepted May 1, 2000.

0037-9727/00/2251-0080\$15.00/0

Copyright © 2000 by the Society for Experimental Biology and Medicine

breeder mice, and the occasional ovarian amyloidosis associated with chronic nephritis (5–9). In those findings the amyloidosis was an uncommon incidental occurrence, and the type of amyloid was not characterized.

Materials and Methods

Animals. A number of strains of wild-derived house mice and inbred laboratory mice were used in the study. The Pas-strain was supplied by Dr. James Pasley (U. of Arkansas, Little Rock, AR), and the Bron-strain was supplied by Dr. Frank Bronson (U. of Texas, Austin, TX). Three other strains of wild-derived house mice, trapped by Dr. Michael Potter in Maryland, were supplied by the wild house mouse colonies at Hazelton Labs, MD. These were the HAF-strain (Haven's Farm), SAF-strain (Sanner's Farm), and JJD-strain (J.J. Downs). Balb/cJ and Balb/cByJ strains of laboratory mice were purchased from Jackson Labs (Bar Harbor, ME). All mice were routinely bred in our mouse colony, and experimental animals were selected from the matings.

Cages. Populations were grown in one of four types of cages: standard 0.045 m² breeding stainless steel cages; 0.48 m² "gang" stainless steel cages; 0.92 m² plexiglass cages for behavioral observations; and 1.82 m² or 3.92 m² double-decked stainless steel or wood-and-screen cages with free access to both levels, as described earlier (2, 10). Living needs were supplied in excess of usage.

Populations. The details of the populations, their types, cage sizes, and demographic data are given in Table I (Pas-strain), Table II (Bron-strain), and Table III (Balb/cJ; Balb/cByJ; HAF-strain; SAF-strain; and JJD-strain). All populations were begun by placing a single male with 2–20 females. The colonizing female mice were reproductively competent and within 2 or 3 days of the same age. Populations were checked daily for litters. Complete censuses were

taken every 3–4 weeks at which times all mice were removed from the cage, adult females palpated for pregnancy, and female offspring toe-clipped for identification. With the exception of population studies D1 and F9 of the Pas-strain, all new males were permanently removed, and populations were raised as single male/all female populations. In population studies D1 and F9, the male offspring were returned, and the populations were raised as mixed populations.

Populations were maintained on a 14:10 daily schedule of white:red light, the former beginning at 1200 hr daily. At the conclusion of each population study, comparable numbers of reference (control) females were also sacrificed. The control animals consisted of virgin females of the same strain and similar ages housed in groups of four, and breeders maintained in breeder cages.

Behavioral Observations. Observations were made under red light on populations housed in plexiglass cages. Observations were of 10–15 min daily for 60 days, and less often thereafter (11). Observations were made between 1000 hr and 1200 hr. Behavioral patterns were recorded as per Chovnick *et al.* (1).

Sample Collections. When populations were terminated, all animals, including controls from the breeding colony, were individually removed from their cages, placed in a jar containing a small amount of ether, and carried to an outside anteroom. Transportation of each mouse to the anteroom took 10–14 sec, by which time the animal was unconscious from exposure to the ether fumes. The animal was removed from the ether jar, quickly weighed, and then decapitated. Trunk blood was collected in heparinized 12 × 75-mm glass test tubes, and then centrifuged. Plasma was removed and stored frozen for later radioimmunoassay of steroid hormones. These results have been presented previously (3). After decapitation, all mice were skinned, organs well exposed, and the carcasses placed in 4% neutral,

Table I. Demographic and Reproductive Data for Pas-Strain Populations, Tabulated with Respect to Cage Size^a

Population	Max. no. in pop.	Max. density (n./m ²)	Duration of study (days)	Sex ratio		Age at pop. termination (days)	Percentage of females w. ovarian lesions	Severity of ovarian lesions ^b
				Start F:M	Finish F:M			
D1*	100	26	565	Cage size = 3.9 m ² 2:1 25:0		378–586	100%	66%
G†	95	53	679	Cage size = 1.8 ² 2:1 90:1		289–700	46%	49%
I†	61	34	464	2:1 47:1		280–485	69%	38%
F9‡	79	86	399	Cage size = 0.9 m ² 2:1 11:15		263–362	0%	0%
F10†	66	72	394	2:1 12:1		297–415	42%	21%
F12†	67	73	397	5:1 54:1		106–418	33%	59%
F14†	58	63	340	5:1 38:1		156–361	8%	15%

^a Pas-strain of *Mus musculus* obtained from Dr. J. Pasley, Little Rock, Arkansas.

^b Given as percentage replacement of luteal tissue with amyloid.

* Raised as a mixed population, but no males survived to termination of study.

† Raised as a predominantly female population with a single stud male. Male offspring were removed at census.

‡ Raised as a mixed population.

Table II. Demographic and Reproductive Data for Bron-Strain Populations, Tabulated with Respect to Cage Size^a

Population	Max. no. in pop.	Max. density (no./m ²)	Duration of study (days)	Sex ratio		Age at pop. termination (days)	Percentage of females w/ ovarian lesions	Severity of ovarian lesions ^b
				Start F:M	Finish F:M			
P8	51	28	592	Cage size = 1.8 m ² 6:1 38:1		253–627	0%	0%
P11	63	68	461	Cage size = 0.9 m ² 6:1 60:1		114–483	10%	14%
P4	73	152	434	Cage size = 0.48 m ² 20:1 64:1		435–632	17%	50%
P9*	43/53	956/110	590	2:1	51:1	139–717	41%	35%

^a Bron-Strain of *Mus musculus* obtained from Dr. F. Bronson, Austin, Texas. Populations were raised as predominantly female populations with one stud male. Male offspring were removed at census.

^b Given as percentage replacement of luteal tissue with amyloid.

* Population started in a 0.045 m² cage and transferred to a 0.48 m² cage; max. no. and density are given as values in smaller cage/values in larger cage.

Table III. Demographic and Reproductive Data for Nine Separate Population Studies of Two Strains of Laboratory Mice (Balb/cJ; Balb/cByJ) and Three Strains of Wild House Mice (HAF-Strain; SAF-Strain; JJD-Strain)^a

Mouse strain	Population	Cage size	Max. no. in pop.	Max. density (no./m ²)	Duration of study (days)	Sex ratio		Age at pop. termination (days)	Percentage of females w/ ovarian lesions	Severity of ovarian lesions ^b
						Start F:M	Finish F:M			
Balb/cJ	P1	.48 m ²	32	67	536	20:1	21:0	426–587	0%	0%
	P2	.48 m ²	22	46	522	20:1	9:1	552–573	0%	0%
	P17*	.48 m ²	6	13	300	5:1	3:0	434	0%	0%
Balb/cByJ	P14	3.95 m ²	46	12	554	5:1	34:0	376–636	0%	0%
HAF	P5†	.48 m ²	11	23	534	10:1	8:1	594–648	13%	20%
	P13	1.82 m ²	38	21	599	5:1	35:0	138–689	0%	0%
SAF	P6‡	.48 m ²	9	19	534	8:1	1:0	591	100%	25%
JJD	P7*	.045 m ²	3	67	226	2:1	0:1	—	—	—
	P16¶	.48 m ²	15/19	31/10	448	3:1	19:0	190–557	0%	0%

^a Populations were raised as predominantly female populations with one stud male. Male offspring were removed at census.

^b Given as percentage replacement of luteal tissue with amyloid.

* Population had no recorded births.

† Population had no surviving litters. One of eight surviving original females had ovarian lesions.

‡ Population had no recorded births. The one surviving original female had ovarian lesions.

¶ Population started in a .48 m² cage and transferred to a 1.82 m² cage; max. no. and density are given as values in smaller cage/values in larger cage.

buffered paraformaldehyde. Later, selected organs were dissected out, weighed, and then prepared for histologic analyses.

Preparation of Tissues for Light Microscopy.

Paraffin-embedded tissues were sectioned at 5 µm and routinely treated with the following stains: hematoxylin-eosin and PAS-hematoxylin; Congo red, plus or minus pretreatment with potassium permanganate (12, 13); thioflavin-T; Mallory's trichrome and van Gieson's stains for connective tissue; Verhoeff's Orcein stain for elastica; Oil-Red-O for fat; and Prussian Blue for iron pigments. Tissues stained with Congo red were examined under polarized light. Tissues stained with thioflavin-T as well as those stained with Congo red were examined with UV light (amyloid fluoresces white with thioflavin-T and orange with Congo red).

Ovarian lesions were graded as follows: the percentage replacement of corpora lutea with amyloid and necrotic ma-

terial was estimated for individual corpora lutea, and averaged to give a figure for total replacement in each section. This figure was multiplied by the percentage of ovary containing corpora lutea. The final number yielded the percentage of amyloid-necrotic replacement for the whole ovary. Grading was repeated a number of times, and the grades were reproducible within 10% or less.

Preparation of Tissue for Electron Microscopy.

Lesioned ovaries were cut into 1-mm cubes and placed in a chilled primary fixative solution of 4% paraformaldehyde with 2% glutaraldehyde for 2 hr. The pH of the solution was 7.2 and isoosmolar to serum (14). After postfixation in a 1% solution of osmium tetroxide for 1 hr and dehydration in acetone, the cubes were embedded in standard grade epon and sectioned using an American Optical (TM) ultra-microtome. Routine thick sections were cut and viewed with light microscopy for orientation. The ultra-thin

sections were stained using uranyl acetate for 20 min and lead citrate for 5 min (15). Thin sections were examined with either a Phillips TM 201 or a Hitachi Y TM H-7000 electron microscope.

Characterization of Ovarian Amyloid. Lesioned ovaries of Pas-strain females, from population studies D1 and G, and lesioned ovaries, from Bron-strain females from population studies P9 and P4, were processed together with sections of human liver tissue containing AA amyloid, as well as with human brain with Alzheimer's disease (Supplied by Dr. James Goldman, Department of Pathology, Columbia College of Physicians & Surgeons, NY). All tissues were analyzed for the presence of AA amyloid by a peroxidase-antiperoxidase (PAP) procedure that combined the methods of Weidemann *et al.* (16), Koo *et al.* (17), and Martin *et al.* (18). The B/A₄ antibodies used in the procedure (Purchased from Boehringer-Mannheim Corp.) react with Alzheimer's precursor protein A₄, and were derived from mouse-mouse hybrid cells. The B/A₄ antibodies also cross-react with AA amyloid from fish, rat, mouse, and monkey. Microscope slides containing the paraformaldehyde-fixed, paraffin-embedded ovarian sections were placed in toluene, and then sequentially run down through alcohols to water. Then, following pretreatment with 15% formic acid (19) the sections were treated with rabbit serum to block nonspecific staining; incubated with monoclonal antipre-B/A₄ antibody; and, washed in buffer. Next, the sections were treated with biotinylated, mouse-adsorbed, rat anti-mouse IgG purchased from Vector Laboratories. After endogenous peroxidase was quenched with 0.3% hydrogen peroxide in methanol, the sections were treated with the biotin-avidin PAP complex, and then incubated in diaminobenzidine chromogen solution for 2–7 min. Slides were washed in distilled water, counterstained with Harris Hematoxylin for 30 sec, dehydrated, cleared with xylene, and

then coverslipped. Sections were examined for a positive chromogen reaction indicative of AA amyloid deposition.

Statistical Analyses. All replicate data were subjected to ANOVA and Student's *t* test.

Results

Demographic Analyses. In all population studies, maximum population size was reached in 120–180 days. Population growth typically involved a rapid phase that was followed by slower growth. The slower rate of growth was always initiated by a change in female behavior, first noted as a pronounced shift in social organization. Where earlier in the population the females had mated, delivered their young, and raised their litters, as the population increased in size, the females gradually stopped mating and began to chase and fight with both male and female "intruders." From that point on, there was no increase in population size. The males in the populations became severely wounded. In population D1, a mixed population, all males were eventually killed by the females. In population I, the single stud male was seriously wounded in the posterior region and eventually lost its tail. When the populations were terminated, the vast majority of the females were still ovulating, as judged by the presence of corpora lutea. Most females had large numbers of uterine placental scars, suggesting that they had been pregnant repeatedly, but had either aborted or resorbed their embryos. For a recent review of this phenomenon, see Clark *et al.* (20).

Figure 1 is a plot of the history of population I (male removal population). Note that the first records of male and female wounds were on Day 144 and Day 168, respectively. Note also that after Day 160, only one of the litters that was born survived. As in all population studies, female aggression, once initiated, continued unabated until the population was terminated, which in population I was at 464 days. At

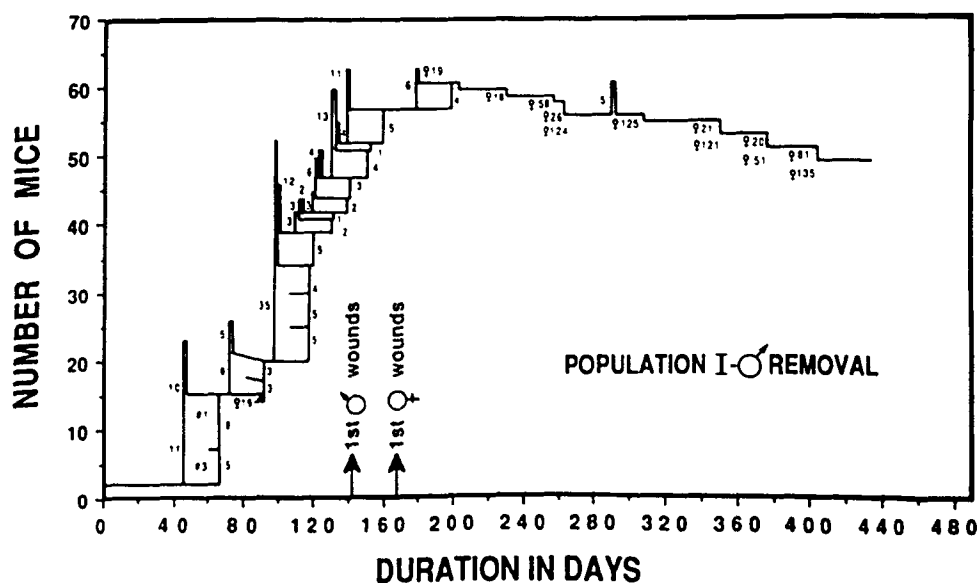


Figure 1. Plot of the history of mouse Population I. The population was started at Day 0 by placing two female and one male weanling mice in a 1.82 m² cage. Subsequent litters are plotted as vertical rises, with the number of pups in each litter indicated on the left side of each rise. Male offspring were weaned at census and permanently removed from the population. The number of remaining females in each litter are indicated on the right side of each rise. The numbers in the first "boxes" (#1 and #3) are the identification numbers of the founding females. Identities of subsequent dams are not indicated. First wounds are indicated by arrows. Deaths are denoted by vertical drops, with the identity of the dead individuals indicated. Note that only two litters were born after Day 160. Population I was terminated on Day 464.

its maximum size, population I contained 60 females and the single stud male. At autopsy it was revealed that a significant number of the females had grossly enlarged ovaries, due to the presence of one, or more, large amorphous masses. Examination of these ovaries *via* light microscopy indicated that the masses, or lesions, were originally corpora lutea, but now contained an accumulation of membrane fragments and other cellular debris suggestive of incomplete luteolysis.

Table I contains the demographic and reproductive data for all Pas-strain population studies, including population I, tabulated with respect to cage size. As indicated, 69% of the females in population I had lesioned ovaries. Further analyses indicated that 38% of normal luteal tissue had been replaced by the lesion. In population study D1, the population reached a maximum size of 100 animals. When the study was terminated at 565 days there were 25 surviving females and no surviving males. All females had lesioned ovaries. In addition, two-thirds of normal luteal tissue in each ovary had been replaced by the lesion. Population G was another study of Pas-strain mice that yielded significant numbers of females with lesioned ovaries. When population G was terminated at 679 days, there were 90 surviving females. Forty-six percent of these animals had lesioned ovaries. In the remaining F series of population studies of the Pas-strain mice, F9 through F14, the populations were all raised in smaller cages and for shorter periods of time. In these smaller cages, the populations reached higher maximum population densities, but there were fewer females with lesioned ovaries. The average maximum population density for all population studies of the Pas-strain of mice was 57 animals/m².

Table II contains the demographic and reproductive data for the Bron-strain population studies. As indicated, few of these populations produced significant numbers of females with lesioned ovaries. This was most evident when populations were raised in the same-sized cages as the Pas-strain and for the same duration; however, when the Bron-strain females were housed in the smaller 0.045 m² and 0.48 m² cages, a number of the females developed lesioned ovaries. Population P9 was started in a 0.045 m² cage with two females and a single stud male. A number of births were recorded, and after 160 days, there were 43 females in the population. The 43 females and the single stud male were subsequently transferred to a larger 0.48 m² cage. Shortly thereafter, a few females produced litters. However, litter production in the larger cage was short-lived, and it soon

ceased. When population P9 was terminated after an additional 434 days, there were 53 surviving females. At autopsy, 41% of the females had lesioned ovaries.

Table III contains the demographic and reproductive data from population studies that were conducted on two strains of inbred laboratory mice and three strains of wild-derived house mice. As in the Pas-strain and Bron-strain animals, the populations of female inbred laboratory mice (Balb/cJ and Balb/cByJ) became aggressive as population size increased, and they subsequently ceased mating; however, in contrast to the Pas-strain and Bron-strain animals, none of the female laboratory mice developed ovarian lesions.

Population studies that were conducted on the three wild-derived strains of house mice initially produced very little reproductive and demographic data. In population study P5 of the HAF-strain, only three litters were produced, and none survived to the next census. When P5 was terminated after 534 days, one of the eight surviving original P5 females had ovarian lesions. In population study P6 (SAF-strain), there were no recorded births. The lone surviving original female had ovarian lesions. Population study P7 (JJD-strain) had no recorded births and no surviving original females. Population studies of the HAF-strain and JJD-strain were subsequently repeated with second-generation animals from the breeding colony. In contrast to the initial population studies, the second-generation females mated and reproduced. However, none of the females developed ovarian lesions. In population study P13 (HAF-strain), none of the 35 females had ovarian lesions, even after 599 days. In population study P16 (JJD-strain), all 19 surviving females had normal ovaries after 448 days. As in many population studies, the females in P13 and P16 killed the stud males.

Table IV contains the average weights of selected organs from Pas-strain breeder and population females. As indicated, the population females had thymus glands and uteri that weighed significantly less than the same organs from breeder females of the same strain. In contrast, the adrenal glands from the population females weighed significantly more than the adrenal glands from breeder females.

With the exception of population study F11 (Pas-strain), lesioned ovaries were larger and weighed more than the nonlesioned ovaries. In population F11, the lesioned ovaries weighed the same as the nonlesioned ovaries. Statistical analyses were performed on selected organ weights

Table IV. The Average Weights of Selected Organs from all Pas-Strain Population Females^a

Animals	Thymus	Spleen	Adrenals	Uterus	Ovaries
Population females (321) ^b	19 ± 2	124 ± 13	7.6 ± 0.3*	67 ± 6	13.5 ± 1.2
Breeder females (18)	40 ± 13†	174 ± 36	6.4 ± 0.4	162 ± 50†	15.4 ± 6.3

^a Organ weights in mg ± SEM. Adrenals and ovaries are paired weights.

^b Number of animals in each group.

* Value significantly greater ($P < 0.05$).

† Value significantly greater ($P < 0.001$).

from population studies G and I of the Pas-strain, and P9 of the Bron-strain, and are representative of all populations of animals in which there was a significant incidence of ovarian lesions. Note in Table V that the average weight of lesioned ovaries in the Pas-strain populations G and I was double that of the nonlesioned ovaries. In population P9 of the Bron-strain, the lesioned ovaries weighed one-third more than the nonlesioned ovaries. With the exception of spleen weights from females in population G (Pas-strain), there were no other statistical differences in organ weights between females having and not having lesioned ovaries.

Shown in Table V are the average ages of females with, and without, lesioned ovaries. As indicated, the average age of females with and without lesioned ovaries in the Pas-strain was 450 days vs 342 days in population G, and 377 days vs 356 days in population I, respectively. In the Bron-strain population, P9, the average age of females with and without lesioned ovaries was 356 days vs 365 days, respectively.

The overall incidence of females with lesions and the severity of the lesions with respect to the age of the animal and duration of the experiment were calculated for the Pas-strain (data from mixed population F9 was not used). In populations D1, G, I, and F10 through F14 (Table I) the prevalence of ovarian lesions was positively correlated with the duration of experiments in days ($r = 0.820$, $n = 10$, $P < 0.01$). In considering the total number of individual mice with lesions, the severity of the lesions was significantly correlated with age/duration ($n = 143$, $P < 0.0001$).

In the Bron-strain, the mean prevalence of lesions per cage size was highly correlated with the logarithms of cage size ($n = 4$, $r = 0.995$, $P < 0.01$), as were the mean frequencies of lesions in individual populations ($n = 10$, $r = 0.884$, $P < 0.01$). The mean severity of lesions per cage size also was highly correlated with logarithms of cage size ($n = 4$, $r = 0.980$, $P < 0.05$), as were the mean severity of lesions per ovary per population ($n = 10$, $r = 0.743$, $P < 0.02$).

Histologic Analyses of Lesioned Ovaries. Figure 2 is a photographic plate of four light micrographs of tissue cross sections of a nonlesioned ovary and lesioned

ovary. Micrographs 2A and 2B demonstrate the cellular integrity typically found in a corpus luteum (CL), and micrographs 2C and 2D demonstrate the lack of cellular integrity typically found in a lesion (L). Figure 3 is a photographic plate of four light micrographs of a lesioned ovary at higher magnification. Micrograph 3A shows a CL being replaced by amyloid and necrotic debris. Note the nearly occluded thecal artery (a) surrounded by PAS + amyloid fibrils. The arrow points to other amyloid fibers. Micrograph 3B shows one CL entirely replaced by amyloid (upper right), and an adjacent CL with a more recent amyloid replacement (arrow). Micrograph 3C is a higher magnification showing early amyloid replacement in a CL. Note the artery with greatly thickened walls. Membranes have disappeared from the periphery of one area (arrow). Note also the amyloid that extends into the surrounding tissue (lower right). Micrograph 3D is a higher magnification showing progression of amyloid replacement in a CL. Thecal arteries are nearly obliterated. Note the absence of a clear-cut boundary between the amyloid and luteal cells (arrow).

Figure 4 is a photographic plate of four electron micrographs of increasing magnification of a thin section of a lesioned ovary. Micrographs 4A and 4B demonstrate the luteal cell membrane disruption and attendant lack of cellular structure that is associated with the formation of the lesion. Micrographs 4C and 4D show the bundles of amyloid fibers that surround a small blood vessel near the lesion.

Typically, amyloid is first detected in thickened walls and reduced lumen of thecal arteries located in the intima and smooth muscle. The amyloid is next seen dispersing into adjacent thecal tissue, with the subsequent invasion of the CL proper. As the amyloid extends from the theca into the CL, the number of fibrils decreases rapidly. Luteal cells not in contact with the amyloid "front" appear to be normal. Luteal cells that are in contact with the amyloid "front," in contrast, no longer have intact membranes, and organelles are seen flowing into the surrounding material. Necrosis and loss of luteal cells proceeds until the CL is replaced by a "hyaline" mass of necrotic debris, amyloid, and probably serum components. Trapped cellular elements are eventually lysed and disappear. The whole mass becomes electron

Table V. The Average Age of the Animals and the Weights of Selected Organs from Females With, and Without, Lesioned Ovaries in Population G (Pas-Strain), Population (Pas-Strain), and Population P9 (Bron-Strain)^a

Animals	Age	Thymus	Spleen	Adrenals	Uterus	Ovaries
G w/lesions (39) ^b	450 ± 12*	21.8 ± 2	165.0 ± 18*	6.6 ± 0.2	43.9 ± 4	12.1 ± 1†
w/o lesions (46)	342 ± 18	21.4 ± 1	102.0 ± 15	6.9 ± 0.2	32.5 ± 5	5.0 ± 0.3
I w/lesions (31)	377 ± 6	15.9 ± 2	158.9 ± 16	7.5 ± 0.4	80.8 ± 10	23.9 ± 2†
w/o lesions (14)	356 ± 10	12.5 ± 2	148.9 ± 25	7.1 ± 0.3	61.7 ± 9	10.5 ± 1
P9 w/lesions (20)	356 ± 17	20.5 ± 2	40.2 ± 2	8.3 ± 0.3	nd	11.3 ± 1*
w/o lesions (29)	365 ± 27	20.9 ± 2	38.8 ± 3	8.7 ± 0.4	nd	8.5 ± 0.7

^a Age in days ± SEM and organ weights in mg ± SEM. Adrenals and ovaries are paired weights.

^b Number of animals in each group.

* Value significantly greater ($P < 0.05$).

† Value significantly greater ($P < 0.001$).

nd = not determined.

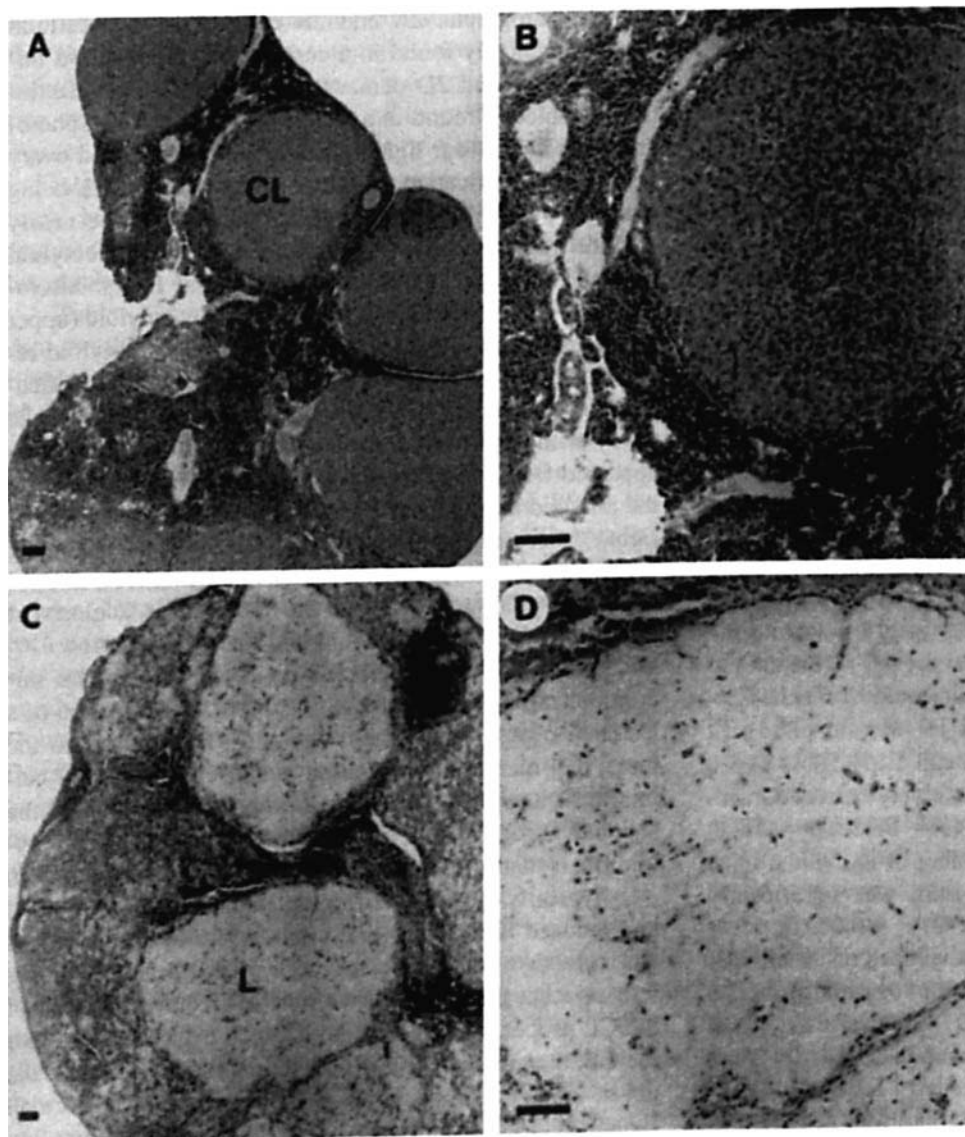


Figure 2. Light micrographs of normal and lesioned ovaries. (A) Low magnification of cross-section of normal ovary showing five recent corpora lutea (CL). (B) Higher magnification of individual corpus luteum in normal ovary showing the typical cellular structure. (C) Low magnification of cross section of lesioned ovary showing two white, amorphous, lesions (L). (D) Higher magnification of individual lesion showing the absence of cellular structure. Hematoxylin & eosin; Scale bars, 100 μ m.

lucent without structure or recognizable components and highly resistant to staining. In no instances are there any signs of an inflammatory reaction.

Histochemical Analyses of Lesioned Ovaries. Tissue sections of lesioned ovaries that were stained with Congo red and then visualized with polarized light showed a high degree of birefringence in specific areas. This localized birefringence was due to isolated individual cells lining the vascular sinusoids. A similar distribution was observed when the lesioned tissue sections were stained with thioflavin-T, and then visualized with UV light. Treatment of tissue sections with potassium permanganate *did not* block tissue staining with Congo red, suggesting that the amyloid is a primary amyloid. As positive control for this staining protocol, and in contrast with the ovarian amyloid, treatment of human AA amyloid tissues with potassium permanganate *did* block staining with Congo red. In addition, B/A₄ antibody *did not* react with the ovarian amyloid, but *did* react with human AA amyloid tissues. Finally, in all

histochemical analyses, the strongest amyloid reaction was found in the walls of thecal arteries and in the single lining of cells of the luteal sinusoids. Lesser amyloid reactions were found in the theca and periphery of the CL.

Histologic and Histochemical Analyses of Other Tissues. Analyses of tissue sections of uteri from Pas-strain and Bron-strain females indicated the presence of secondary amyloidosis of medium-sized muscular arteries of the mesometrium, metrial triangle, and myometrium in 23 of the 412 mice examined. The uterine lesions were associated with acute or chronic necrotizing arteritis accompanying inflammatory responses to dead embryos. Analysis of kidney tissue from these same experimental mice indicated that over 80% of the animals had either subacute, chronic, or old healed pyelonephritis. The pyelonephritic lesions ranged from minimal to end-stage kidney. The severity of renal lesions was significantly correlated with severity of ovarian lesions ($n = 175$, $r = 0.204$, $P < 0.01$), but this relationship accounted for only 4% of the variance

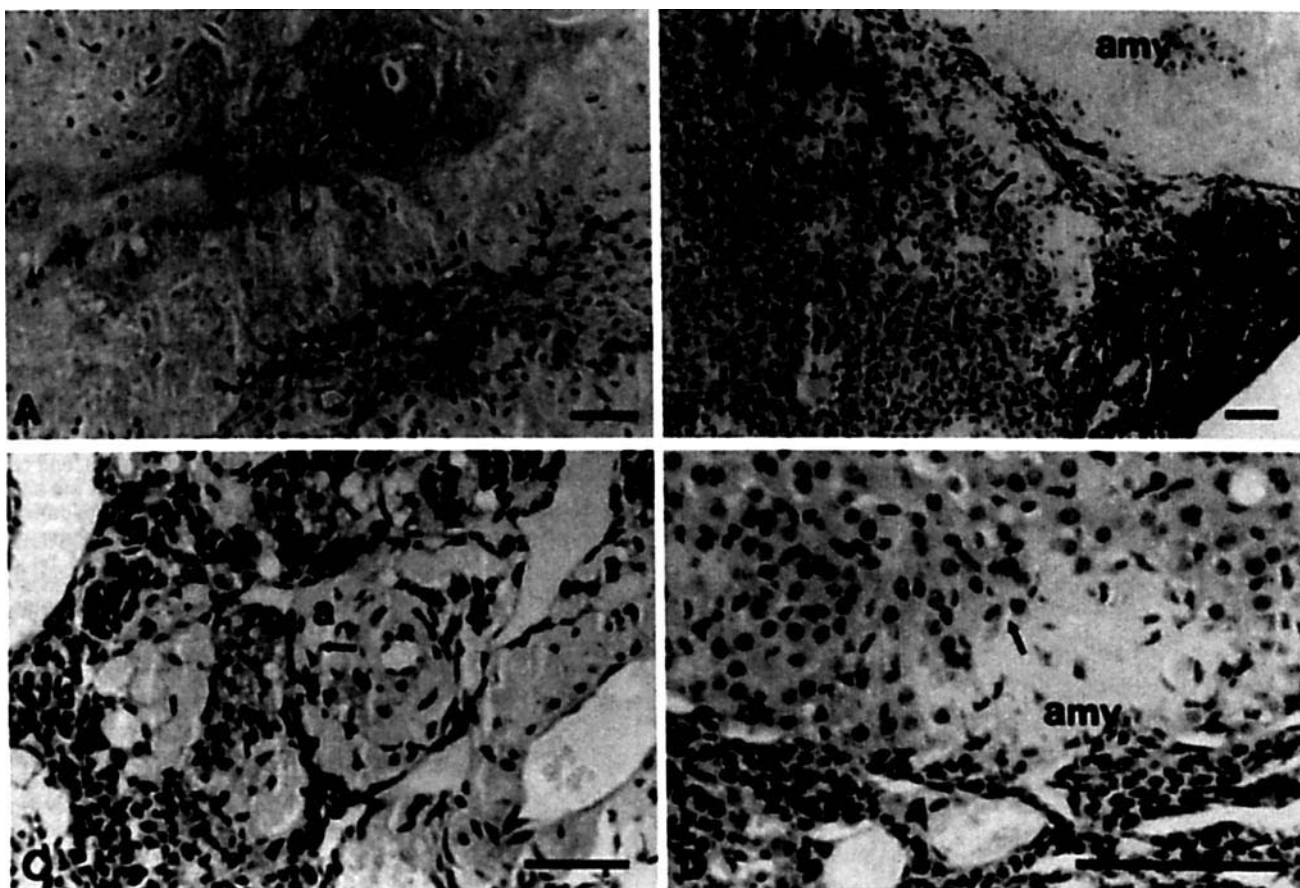


Figure 3. Light micrographs of lesioned ovary. (A) Cross section showing a CL being replaced by amyloid and necrotic debris. Note the nearly occluded thecal artery (a) surrounded by PAS + amyloid fibrils. Arrow points to other amyloid fibrils. PAS-hematoxylin. (B) Cross section showing one CL entirely replaced by amyloid (amy). An adjacent CL contains a more recent amyloid replacement (arrow). PAS-hematoxylin. (C) Cross section showing early amyloid replacement in a CL. Note the artery (a) with greatly thickened walls. Membranes have disappeared from the periphery of one area (arrow). Note also the amyloid that extends into the surrounding tissue (lower right). Hematoxylin & eosin. (D) Cross section showing progression of amyloid replacement in a CL. Thecal arteries are nearly obliterated. Note the absence of a clear-cut boundary between the amyloid (amy) and luteal cells (arrow). Hematoxylin & eosin. Scale bars, 100 µm.

and could reflect the increase in severity of both diseases with time (age). In addition, there was an apparent absence of ovarian disease in 32 mice with renal disease and an absence of renal lesions in 16 mice with ovarian lesions. Although some very early renal and ovarian lesions could have been missed, these data indicate that pyelonephritis and ovarian amyloidosis were not directly related.

Discussion

The Pas-strain of wild mice had the greatest predisposition toward the development of ovarian lesions. A number of the Pas-strain females actually had lesioned ovaries by 250 days of age, suggesting that the pathology is not strictly an effect of senescence. The development of the lesion in the Pas-strain was independent of cage size. In the Bron-strain, in contrast, the size of the cage was critical. This was demonstrated most effectively in population study P9, where animals initially housed in a small 0.045 m² cage for 160 days had the highest incidence of ovarian lesions. In population studies of the Balb/cJ and Balb/cByJ laboratory

mice, and the HAF-strain, SAF-strain, and JJD-strain wild house mice, only two females developed ovarian lesions. This tentatively suggests that these strains are not predisposed to develop ovarian lesions. However, we cannot rule out the effect of limited cage size in these strains. In population study P7 of the JJD-strain, the animals were initially housed in a small 0.045 m² cage, as in population study P9 (Bron-strain). However, none of the colonizing females in P7 gave birth, and all were dead by 226 days. This study was not repeated in the small 0.045 m² cage. All further population studies of the Balb/cJ and Balb/cByJ laboratory mice, and the HAF-strain, SAF-strain, and JJD-strain wild house mice were conducted in larger cages.

The failure of normal luteolysis, especially in older females, is of unknown etiology at this time. Whether it is the result, or precedes amyloid formation, is unclear. Female house mice that are housed under crowded conditions are known to exhibit irregular or prolonged estrous cycles (21–24). Animal crowding is considered to be a stressful factor (25, 26) suggesting the possible involvement of the

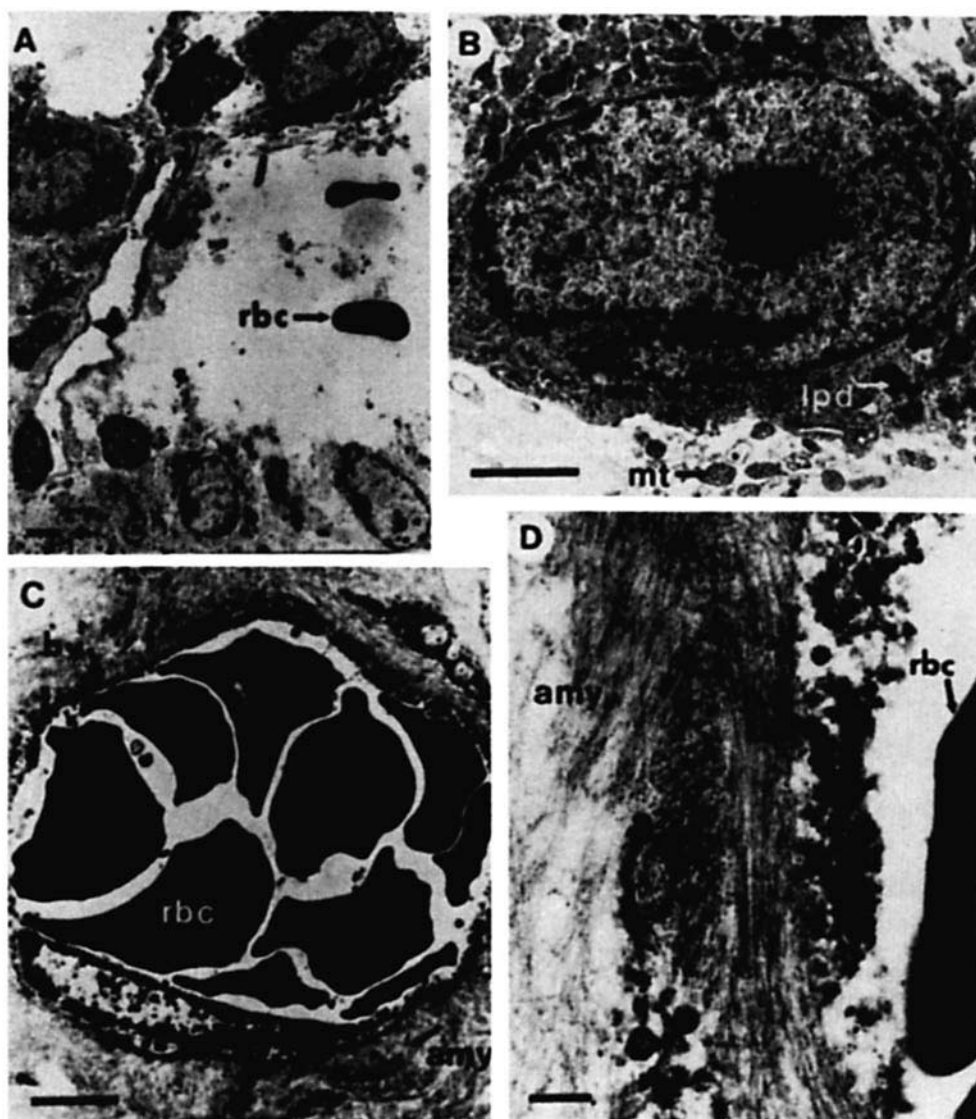


Figure 4. Electron micrographs of lesioned ovary. (A) Area of lesion adjoining a CL showing luteal cell membrane disruption. Cytoplasmic organelles are seen escaping these cells into the clear space. The clear space also contains red blood cells (rbc) and fragments of destroyed cells. (B) Higher magnification of luteal cell bordering lesion. Mitochondria (mt), lipid droplets (lpd), and other cytoplasmic organelles are shown pouring out the lower side of the cell. The nuclear membrane in the same area appears to be disrupted, but no nucleoplasm is escaping. (C) Section through a small blood vessel (bv) near lesion showing darkly stained red blood cells (rbc). Bundles of amyloid fibers (amy) are shown in this micrograph, surrounding the blood vessel and stretching away from it. (D) Micrograph of a portion of the blood vessel showing a higher magnification of the amyloid fibers (amy). Visible on the right is a red blood cell (rbc). Scale bars for A, B, and C, 1 μ m. Scale bar for D, 0.1 μ m.

adrenal gland. In a recent study, adrenalectomized female house mice given corticosterone (B) replacement had suppressed estrous cycles when housed under crowded conditions, whereas adrenalectomized animals without B replacement had regular estrous cycles (27). The overall results of the study led these investigators to suggest that urinary metabolites of B, acting as pheromones in the urine, increase the length of the estrous cycle.

A number of reports have indicated that the weight of the adrenal glands is increased in group-housed female mice (28–31). In our studies, population females had adrenal glands that weighed significantly more than the adrenal glands from breeder females of the same strain (Table IV). Increased adrenal weight is correlated with elevated adrenal activity (30, 32–34). The population females had stress levels of circulating B (3).

Activated T lymphocytes and macrophages play a critical role in luteolysis, contributing to the prompt regression of corpora lutea (35–42). When females have a paucity of immune cells, as in the congenitally athymic nude mouse,

the corpora lutea persist for a long time (43, 44). In the current study, the incomplete luteolysis and the development of ovarian lesions in the population females could be due, at least in part, to reduced levels of activated lymphocytes and macrophages. Stress levels of adrenal steroids have a profound and deleterious effect on the immune system. Glucocorticoids, for example, (i) cause the apoptosis (cell death) of lymphocytes in thymus and liver (45); (ii) inhibit the expression of interleukin-1 β mRNA and interleukin-6 mRNA in macrophages (46); (iii) depress the phagocytic activity and inhibit the release of tumor necrosis factor- α in macrophages (47, 48); and (iv) reduce the activity of manganese superoxide dismutase and glutathione peroxidase in macrophages (49). In the current study, thymus glands from population females weighed significantly less than thymus glands from breeder females (Table IV), the possible consequence of the high levels of B.

Lesioned ovaries weighed significantly more than non-lesioned ovaries (Table V), as a result, presumably, of the incomplete luteolysis and amyloid deposition. Chronic so-

cial strife and repeated pregnancies appear to be an ingredient in the development of the amyloid. Social stress has been reported to augment casein-induced AA amyloid formation, although the effect may actually be due to wounding (50, 51). Wounds from fighting have been reported to cause secondary amyloidosis in group-caged mice (50). In the current study, no such relationship could be established between wounding and ovarian amyloidosis. AA amyloidosis is commonly associated with pyelonephritis and chronic inflammation (7, 52). It is possible that ovarian and renal lesions could co-occur without a direct relationship to each other, but an indirect effect is suggested by the positive correlation between the severity of renal and ovarian lesions. Although AA amyloidosis was rare in our mice, primary amyloid formation may be affected by similar factors. Resistance to azocasein-induced AA amyloidosis in CE/J inbred mice is reported to be due to the production of a genetically determined novel SAA protein (53), but whether or not this bears on ovarian primary amyloidosis is conjectural. A number of studies have examined the effects of steroid hormones on AA amyloidosis, both spontaneous and experimentally induced. However, the results are equivocal. Steroid hormones have been reported to block formation of amyloid, to precipitate it, and to enhance it (54–58). In any event, results from experiments on AA amyloidosis may have little bearing on ovarian primary amyloidosis. The ovarian amyloid is permanganate-resistant and does not cross-react with human B/A₄ amyloid, suggesting that the ovarian amyloid is not an AA amyloid. With respect to its pathogenesis, many questions still remain.

The authors gratefully acknowledge Mr. Henry Eichelberger, of our EM facility, for his assistance in the preparation of the photomicrographs used in this manuscript, and Mr. Mitchell Chorost for his assistance in the population studies.

1. Chovnick A, Yasukawa NJ, Monder H, Christian JJ. Female behavior in populations of mice in the presence and absence of male hierarchy. *Aggressive Behav* 13:367–375, 1987.
2. Yasukawa NJ, Monder H, Leff FR, Christian JJ. Role of female behavior in controlling population growth in mice. *Aggressive Behav* 11:49–61, 1985.
3. Chapman JC, Christian JJ, Pawlikowski MA, Michael SD. Analysis of steroid hormone levels in female mice at high population density. *Physiol Behav* 64:529–533, 1998.
4. Barlow SM, Morrison PJ, Sullivan FM. Effects of acute and chronic stress on plasma corticosterone levels in the pregnant and nonpregnant mouse. *J Endocrinol* 66:93–99, 1975.
5. Deringer MK. Necrotizing arteritis in strain BL/De mice. *Lab Invest* 8:1461–1465, 1959.
6. Dickie MM, Atkinson WB, Fekete E. The ovary, estrous cycle, and fecundity of DBA X CE and reciprocal hybrids in relation to age and the hyperovarian syndrome. *Anat Rec* 127:187–199, 1957.
7. Dunn TB. Amyloidosis in mice. In: Cotchin E, Foe FJ, Eds. *Pathology of Lab Mice and Rats*. Philadelphia: F. A. Davis Co, pp182–212, 1967.
8. Fekete E. A comparative study of the ovaries of virgin mice of the DBA and C57 black strains. *Cancer Res* 6:263–269, 1946.
9. Richardson FL, Hall G. Mammary tumors, mammary gland development, and morphology of ovaries in virgin of strains C3H, CBA, and their F1 hybrids. *J Natl Cancer Inst* 31:529–540, 1963.
10. Christian JJ. Adrenal and reproductive responses to population size in mice from freely growing populations. *Ecology* 37:258–273, 1956.
11. Lloyd JA, Christian JJ. The relationship of activity and aggression to density in two confined populations of house mice (*Mus musculus*). *J Mammal* 48:262–269, 1967.
12. van Rijswijk MH, van Heusden GJ. The potassium permanganate method for differentiating amyloid AA from other forms of amyloid in routine laboratory practice. *Am J Pathol* 97:43–58, 1979.
13. Wright JR, Calkins E, Humphery RL. Potassium permanganate reaction in amyloidosis: A histologic method to assist in differentiating forms of this disease. *Lab Invest* 36:274–281, 1977.
14. Glauert AM. Fixatives. In: Glauert AM, Ed. *Practical Methods in Electron Microscopy*, Vol 3. Amsterdam: North-Holland Publishing Co., pp5–72, 1974.
15. Knight DP. Cytological staining methods in electron microscopy. In: Glauert AM, Ed. *Practical Methods in Electron Microscopy*, Vol 5. Amsterdam: North-Holland Publishing Co., pp25–76, 1977.
16. Weidemann A, Konig G, Bunke D, Fischer P, Salbaum JM, Masters CL, Beyreuther K. Identification, biogenesis, and localization of precursors of Alzheimer's disease A4 protein. *Cell* 57:115–126, 1989.
17. Koo EH, Sisodia SS, Archer DR, Martin LJ, Weidemann A, Beyreuther K, Fischer P, Masters CL, Price DL. Precursor of amyloid protein in Alzheimer's disease undergoes fast anterograde axonal transport. *Proc Natl Acad Sci U S A* 87:1561–1565, 1990.
18. Martin LJ, Sisodia SS, Koo EH, Cork LC, Dellovade TL, Weidemann A, Beyreuther K, Masters C, Price DL. Amyloid precursor protein in aged nonhuman primates. *Proc Natl Acad Sci U S A* 88:1461–1465, 1991.
19. Vinters HV, Pardridge WM, Secor DL, Ishii N. Immunohistochemical study of cerebral amyloid angiopathy: II. enhancement of immunostaining using formic acid pretreatment of tissue sections. *Am J Pathol* 133:150–162, 1988.
20. Clark DA, Arck PC, Chaouat G. Why did your mother reject you? Immunogenetic determinants of the response to environmental selective pressure expressed at the uterine level. *Am J Reprod Immunol* 41:5–22, 1999.
21. Lee S, van der Boot LM. Spontaneous pseudopregnancy in mice. *Acta Physiol Pharmacol Neerl* 4:442–443, 1955.
22. Lee S, van der Boot LM. Spontaneous pseudopregnancy in mice II. *Acta Physiol Pharmacol Neerl* 5:213–214, 1956.
23. McClintock MK. Pheromonal regulation of the ovarian cycle: Enhancement, suppression, and synchrony. In: Vandenbergh JG, Ed. *Pheromones and Reproduction in Mammals*. New York: Academic Press, pp113–149, 1983.
24. Whitten WK. Pheromones and mammalian reproduction. In: McLaren A, Ed. *Advances in Reproductive Physiology*. New York: Academic Press, Vol 1:pp155–177, 1966.
25. Christian JJ. Phenomena associated with population density. *Proc Natl Acad Sci U S A* 47:428–448, 1961.
26. Christian JJ. Endocrine adaptive mechanisms and the physiologic regulation of population growth. *Physiol Mammal* 1:189–353, 1963.
27. Ma W, Miao Z, Novotny MV. Role of the adrenal gland and adrenal-mediated chemosignals in suppression of estrus in the house mouse: The Lee-Boot effect revisited. *Biol Reprod* 59:1317–1320, 1998.
28. Christian JJ. Effect of population size on the weights of the reproductive organs of white mice. *Am J Physiol* 181:477–480, 1955.
29. Christian JJ. Effect of population size on the adrenal glands and reproductive organs of male mice in populations of fixed size. *Am J Physiol* 182:282–300, 1955.
30. Louch CD, Higginbotham M. The relationship between social rank and plasma corticosterone levels in mice. *Gen Comp Endocrinol* 8:441–444, 1967.
31. Welch BL, Klopfer PH. Endocrine variability as a factor in the regulation of population density. *Am Nat* 95:256–260, 1961.
32. Brain PF, Newell NW. Isolation versus grouping effects on adrenal

- and gonadal function in albino mice I: The male. *Gen Comp Endocrinol* 16:149–154, 1971.
33. Brain PF, Newell NW. Isolation versus grouping effects on adrenal and gonadal function in albino mice II: The female. *Gen Comp Endocrinol* 16:155–159, 1971.
 34. Vandenbergh JG. Eosinophil response to aggressive behavior in CFW mice. *Anim Behav* 8:13–18, 1960.
 35. Adashi EY. The potential relevance of cytokines to ovarian physiology: The emerging role of resident ovarian cells of the white blood cell series. *Endocr Rev* 3:454–464, 1990.
 36. Bagavandoss P, Kunkel SL, Wiggins RC, Keyes PL. Tumor necrosis factor- α : Production and localization of macrophages and T lymphocytes in the rabbit corpus luteum. *Endocrinology* 122:1185–1187, 1988.
 37. Bukovsky A, Presl J, Holub M. The ovarian follicle as a model for the cell-mediated control of tissue growth. *Cell Tissue Res* 236:717–724, 1984.
 38. Brannstrom M, Mayrhofer G, Robertson SS. Localization of leukocyte subsets in the rat ovary during the periovulatory period. *Biol Reprod* 48:277–282, 1993.
 39. Brannstrom M, Giesecke L, Moore IC, van den Heuvel CJ, Robertson SA. Leukocyte subpopulations in the rat corpus luteum during pregnancy and pseudopregnancy. *Biol Reprod* 50:1161–1189, 1994.
 40. Brannstrom M, Pascoe V, Norman RJ, McClure N. Leukocyte subsets in the follicle wall and corpus luteum throughout the human menstrual cycle. *Fertil Steril* 61:488–495, 1994.
 41. Petrovska M, Sedlak R, Nouza K, Presl J, Kinsky R. Development and distribution of the white blood cells within various structures of the human menstrual corpus luteum examined using an image analysis system. *Am J Reprod Immunol* 28:1–4, 1992.
 42. Petrovska M, Dimitrov DG, Michael SD. Quantitative changes in macrophage distribution in normal mouse ovary over the course of the estrous cycle examined with an image analysis system. *Am J Reprod Immunol* 36:175–183, 1996.
 43. Ruitenberg EJ, Berkvens JM. The morphology of the endocrine system in congenitally athymic (nude) mice. *J Pathol* 121:225–229, 1977.
 44. Bukovsky A, Presl J, Holub M. Ovarian morphology in congenitally athymic mice. *Folia Biol (Praha)* 24:442–450, 1978.
 45. Okuyama R, Abo T, Seki S, Ohteki T, Sugiura K, Kusumi A, Kumagai K. Estrogen administration activates extrathymic T-cell differentiation in the liver. *J Exp Med* 175:661–669, 1992.
 46. Katoh N, Ito T. Inhibition by dexamethasone of interleukin-1- β and interleukin-6 expression in alveolar macrophages from cows. *Res Vet Sci* 59:41–44, 1995.
 47. Nakamura Y, Murai T, Ogawa Y. Effect of *in vitro* and *in vivo* administration of dexamethasone on rat macrophage functions: Comparison between alveolar and peritoneal macrophages. *Eur Respir J* 9:301–306, 1996.
 48. Joyce DA, Steer JH, Abraham LJ. Glucocorticoid modulation of human monocyte/macrophage function: Control of TNF- α secretion. *Inflamm Res* 46:447–451, 1997.
 49. Pereira B, Rosa-Luiz-Fernando BP, Safi-Danilo A, Bechara-Etelvino JH, Curi R. Hormonal regulation of superoxide dismutase, catalase, and glutathione peroxidase activities in rat macrophages. *Biochem Pharmacol* 50:2093–2098, 1995.
 50. Page DL, Glenner GC. Social interaction and wounding in the genesis of 'spontaneous' murine amyloidosis. *Am J Pathol* 67:555–570, 1972.
 51. Ebbesen P. Spontaneous amyloidosis in differently grouped and treated DBA/2, BALB/c, and CBA mice and thymus fibrosis in estrogen-treated BALB/c males. *J Exp Med* 127:387–396, 1968.
 52. Dunn TB. Relationship of amyloid infiltration and renal disease in mice. *J Natl Cancer Inst* 5:17–28, 1944.
 53. Sipe JD, Carreras I, Gonnerman WA, Cathart ES, de Beer MC, de Beer FC. Characterization of the inbred CE/J mouse strain as amyloid resistant. *Am J Pathol* 143:1480–1485, 1993.
 54. Polliak A, Laufer A, George R, Fields M. The effect of cortisone on the formation and resorption of experimental amyloid. *Br J Exp Pathol* 54:6–11, 1973.
 55. Svendsen UG. Occurrence of amyloidosis secondary to the induction of experimental hypertension in mice. *Acta Pathol Microbiol Scand A* 85:263–266, 1977.
 56. Latvalahti J. Experimental studies on the influence of certain hormones on the development of amyloidosis. *Acta Endocrinol* 14 (Suppl):16, 3–89, 1955.
 57. Teilum G. Amyloidosis: Origin from fixed periodic acid-Schiff positive reticuloendothelial cells *in loco* and basic factors in pathogenesis. *Lab Invest* 15:98–110, 1966.
 58. Cohen AS. Amyloidosis in association with rheumatoid arthritis. *Med Clin North Am* 52:643, 1968.